

A simple model of the World Trade Center fireball dynamics

Howard R. Baum*, Ronald G. Rehm

*Building and Fire Research Laboratory, National Institute of Standards and Technology,
100 Bureau Drive Stop 8663, Gaithersburg, MD 20899-8663, USA*

Abstract

An analytical model of the initial expansion of a fireball is presented. The model is based on an exact solution of the low Mach number combustion equations in the form initially proposed by the authors. The equations consist of the conservation of mass, momentum, and energy with an isobaric equation of state. The heat release rate is a prescribed spherically symmetric function characterized by a flame expansion velocity, a flame brush thickness that increases with time, and a heat release rate per unit surface area. The introduction of a prescribed heat release rate obviates the need for an explicit turbulence model. Thus, the inviscid forms of the conservation equations can be used in the analysis. The velocity field is decomposed into a spherically symmetric expansion field and a solenoidal component determined by the buoyancy induced vorticity field. The expansion field together with the induced pressure rise and temperature fields are spherically symmetric. However, the buoyancy forces induce vorticity where the temperature changes rapidly and break the spherical symmetry of the velocity field. The solution is used to study the initial expansion of the fireballs generated in the attack on the World Trade Center south tower. Video images are used to estimate the expansion rate of the fireball. This information, when combined with the analysis, leads to an estimate of the fuel consumed in the fireball that is independent of any assumptions about either the initial fuel distribution or the state of the building following the crash. Published by Elsevier Inc. on behalf of The Combustion Institute.

Keywords: Fireball; Fires; Flame spread; Fluid mechanics; Safety

1. Introduction

The dynamics of fireballs have been studied theoretically from a wide variety of perspectives. A recent review of the state of understanding of the hazards associated with the large-scale release of fuels in the atmosphere [1] provides an excellent introduction to this field. The simplest approach,

developed by Fay and Lewis [2], used an integral approach to predict the rise of a spherically shaped fireball. Models of this type provide little or no information about the details of either the fluid mechanics or combustion processes. More recently, detailed computational fluid dynamics (CFD) based numerical simulations employing $k - \epsilon$ turbulence models have been used to study the burning of both single-phase [3] and two-phase [4] burning of liquid and gaseous releases in the atmosphere. These simulations provide a wealth of detail, at the cost of a considerable amount of computation. They also require a large

* Corresponding author. Fax: +1 301 975 4052.

E-mail address: howard.baum@nist.gov (H.R. Baum).

amount of data as input, which may or may not be available when studying a given scenario.

The present work is aimed at the development of a model of intermediate complexity, which is focused on the initial development of the fireball. The flow is decomposed into a dominant spherically symmetric expansion and a solenoidal component determined by the vorticity induced by the buoyancy generated in the expansion process. The low Mach number combustion equations with a prescribed heat source [5] are solved analytically in this geometry. These equations consist of mass, radial momentum, azimuthal vorticity, and energy equations, together with an isobaric equation of state. This is mathematically equivalent to using two components of the momentum equation for an axially symmetric flow, and permits the decoupling of the two flow components in a rigorous way. The heat release rate is characterized by a flame expansion velocity V , a flame brush thickness increasing linearly with time (representing a temporal mixing layer), and a heat release rate per unit area of nominal flame front q . There are no other input parameters needed to define the model, which should enhance its usefulness in practice. Since the mixing of fuel and air is represented by the flame brush, there is no need for an explicit turbulence model, and the original inviscid form of these equations as derived by the present authors is employed in the analysis. This is a non-trivial point, since the use of traditional turbulence models for problems with spherical symmetry is impossible without introducing additional assumptions and parameters into the models [6]. The solutions obtained below are valid for both a completely unbounded scenario or one where the fireball emerges from a vertical wall.

This work was motivated by the World Trade Center (WTC) disaster on 11 September 2001, particularly the collapse of the towers. As is well known now, each tower was first impacted by one of the hijacked Boeing 767 commercial aircraft flying at very high speed relative to the altitude of the collision. Then, fires in each tower, initiated by the impact and the onboard jet fuel acting as an accelerant and sustained by the combustible building contents, weakened the structure. These two insults, initial impact and fires, to each structure resulted in its collapse [7].

The completeness of the devastation of the towers and surroundings, and the need to find survivors and to clear the debris, meant that there was little, beyond a small but adequate selection of steel structural components, remaining upon which to base an investigation. However, this disaster is probably the photographically best documented disaster ever. The photographs and video clips, together with mathematical models describing initial impact, structural strength and stability, and the fires, provide the only means to recreate and to investigate the disaster. Analy-

sis of the fireballs is an excellent example to illustrate the interaction of mathematical models and photographic evidence to “back out” estimates of the amount of fuel consumed by the fireballs. The fireball generated by the impact to the South Tower, WTC2, is the one most frequently seen because it occurred second. However, there is also limited photographic evidence for the first fireball associated with the North Tower, WTC1. Here, we compare our fireball model with those from WTC2.

Clearly, CFD based simulations of the fireballs would also be useful. Indeed, such calculations have been performed [8], with results that visually resemble photographic images of the event. However, as noted above, such calculations require many unverifiable assumptions about both the initial distribution of fuel and the post-collision building geometry. Thus, an independent calculation that places no reliance on such details and the additional uncertainties associated with any CFD simulation would be a valuable addition to our understanding of what transpired on 9/11.

The remainder of the paper is organized as follows: The equations to be solved are presented in the next section. The following two sections develop the solution for the expansion field and the initial development of the vorticity containing field, respectively. Finally, the solutions to the model equations are used to develop a lower bound estimate of the fuel consumed in the South Tower fireball.

2. Mathematical model

The starting point is the equations of motion for a spherical expanding gas driven by a heat release rate per unit volume $Q(r, t)$. The initial expansion is unaffected by gravity or thermal radiation (see the discussion at the end of the paper for a justification of this point) and the mass, momentum, and energy equations take the form:

$$\frac{\partial \rho}{\partial t} + \frac{1}{r^2} \frac{\partial}{\partial r} (\rho v r^2) = 0, \quad (1)$$

$$\rho \left(\frac{\partial v}{\partial t} + v \frac{\partial v}{\partial r} \right) + \frac{\partial p}{\partial r} = 0, \quad (2)$$

$$\rho \left(\frac{\partial h}{\partial t} + v \frac{\partial h}{\partial r} \right) = Q(r, t). \quad (3)$$

Here, ρ is the gas density, v is the radial velocity, p is the local pressure, and h is the sensible enthalpy in the gas. Assuming that an appropriate constant value of the specific heat C_p can be found (note that C_p for nitrogen, the dominant gas by mass, will be within 10% of its midpoint value over the temperature range 300–1500 K [9]), the equation of state can be written as:

$$\rho h = \rho_\infty h_\infty. \quad (4)$$

The volumetric heat release rate is assumed to have the following form:

$$Q = \frac{q}{\sqrt{\pi}\delta(t)} \exp\left[-\frac{(r - Vt)^2}{\delta^2(t)}\right], \quad \delta = \epsilon Vt. \quad (5)$$

Eq. (5) represents an idealized flame brush centered about the nominal front $r = Vt$. The flame front is taken to be a temporal mixing layer in which the front thickness $\delta(t)$ grows linearly with time with the growth rate characterized by the parameter ϵ . The model is not sensitive to the value of this parameter so long as $\epsilon \ll 1$. The choice $\epsilon = 0.1$ is made for all calculations used in this paper. The above set of equations constitutes a model for the fireball dynamics so long as the expansion is entirely symmetric. It can be solved exactly, as shown in the following section.

However, the interaction of the buoyancy with this expansion breaks down the spherical symmetry. It is the generation of vorticity by this process that leads to the global rise of the fireball. To analyze the early stages of this process, it is convenient to introduce the equation governing the azimuthal component of the vorticity $\omega(r, \theta, t)$ directly, rather than work with a second component of the momentum equation. Let θ be the polar angle measured from the positive vertical direction and define $B(r, t) = \rho/\rho_\infty$. Then, neglecting the non-buoyant baroclinic vorticity generation on the grounds that the pressure and density depend only on the radial coordinate, the vorticity equation can be written in the form [10]:

$$\left(\frac{\partial}{\partial t} + v \frac{\partial}{\partial r}\right) \left(\frac{\omega}{Br \sin \theta}\right) = \frac{g}{B^3 r} \frac{\partial B}{\partial r}. \quad (6)$$

Here, g is the magnitude of the gravitational acceleration. Let the vorticity induced components of the velocity in the radial and polar angular directions, respectively, be denoted by u_r and u_θ . The vorticity is defined in terms of these velocity components as follows:

$$\omega = \frac{1}{r} \left(\frac{\partial}{\partial r}(ru_\theta) - \frac{\partial u_r}{\partial \theta}\right). \quad (7)$$

The vorticity induced component of the flow must be divergence free, for consistency with the spherically symmetric expansion. This can be accomplished [11] by introducing a function ψ , defined so that:

$$u_r = \frac{1}{r^2 \sin \theta} \frac{\partial \psi}{\partial \theta}, \quad u_\theta = -\frac{1}{r \sin \theta} \frac{\partial \psi}{\partial r}. \quad (8)$$

For a constant density flow, ψ would be the stream function, a local measure of the mass flow passing through the system. However, in the present case, it is merely the one surviving component of the vector potential, which defines the velocity in a divergence free flow. Finally, combining

Eqs. (7) and (8), the function ψ is determined from the vorticity field through the solution of:

$$\frac{\partial^2 \psi}{\partial r^2} + \frac{\sin \theta}{r^2} \frac{\partial}{\partial \theta} \left(\frac{1}{\sin \theta} \frac{\partial \psi}{\partial \theta}\right) = -r \sin \theta \omega(r, \theta, t). \quad (9)$$

One final point should be noted. The reason the solenoidal velocity (u_r, u_θ) is not included in the analysis of the expansion and the evolution of the vorticity is that early in the expansion these velocity components are quite small, as the solutions developed below demonstrate. Although the vorticity field is quite intense, it is localized in the region bounded by $R = 0$ and the flame brush. The total circulation, which ultimately determines the magnitude of the solenoidal velocity field, is thus also small initially. In fact, when the two components of the velocity field become comparable, the present analysis is no longer valid. It is precisely in this sense that this is a study of the initial expansion of the fireball.

3. Spherical expansion

The starting point for the analysis is the calculation of the expansion velocity v . This is accomplished by noting that multiplying the mass conservation equation (1) by h and adding it to the energy equation (3) yield an expression for the divergence of the velocity field. This is actually a special case of a relation that can be derived for very general fire scenarios [12,13]. In the present circumstances, the result is:

$$\frac{1}{r^2} \frac{\partial}{\partial r}(r^2 v(r, t)) = \frac{Q}{\rho_\infty h_\infty}. \quad (10)$$

This can be immediately integrated with the boundary condition that $v = 0$ at $r = 0$. The result, ignoring terms of $O \exp(-1/\epsilon^2)$, is:

$$\frac{v}{V} = \left(\frac{q}{\rho_\infty h_\infty V}\right) W(R), \quad R = r/Vt, \quad (11)$$

$$W(R) = \frac{1}{R^2} (f_1(R) - f_2(R)), \quad (12)$$

$$f_1 = \left(\frac{2 + \epsilon^2}{4}\right) \left[1 + \operatorname{erf}\left(\frac{R-1}{\epsilon}\right)\right], \quad (13)$$

$$f_2 = \frac{\epsilon}{2\sqrt{\pi}} \left[(1+R) \exp\left(-\left(\frac{R-1}{\epsilon}\right)^2\right)\right]. \quad (14)$$

There are two points worth noting about this result. First, the solution depends on the physical coordinates only in the combination $R = r/Vt$. Second, the normalized velocity depends only on R and the dimensionless energy release parameter $\beta = q/(\rho_\infty h_\infty V)$. This suggests that *all* physical

quantities associated with the expansion depend only on these quantities.

The density ratio $B = \rho/\rho_\infty$ can now be found from the mass conservation equation (1). This equation now takes the form:

$$-R \frac{dB}{dR} + \beta \left(\frac{2}{R} WB + \frac{d}{dR}(WB) \right) = 0. \quad (15)$$

Since $W(R)$ is known, this is a linear equation for B whose solution can readily be found. The dimensionless temperature ratio or enthalpy ratio $H(R) = h/h_\infty$ then immediately follows from the equation of state (4). The result is:

$$B = \exp(-\beta I(R)) = 1/H, \quad (16)$$

$$I = \int_R^\infty \left(\frac{2}{R} W + \frac{dW}{dR} \right) / (R - \beta W) dR. \quad (17)$$

Figure 1 shows the functions $W(R)$ and $H(R)$. The dimensionless velocity achieves its peak value just outside the point where the heat release rate is at its maximum. It falls rapidly to zero inside the mixing zone, vanishing by symmetry at the center of the expanding gas cloud. Outside the mixing zone, the decay is proportional to R^{-2} , since the entire fireball acts as a source of volume. Inside the mixing zone, the enthalpy and temperature reach a plateau value whose peak value depends on the dimensionless heat release rate parameter β . The solutions are quite sensitive to this parameter. The results plotted in Fig. 1 show that if the ambient temperature is 300 K, a change from $\beta = 0.85$ to $\beta = 0.95$ yields a peak temperature increase from about 1200 K to nearly 1700 K. In contrast to the velocity profile, the temperature decays sharply to its ambient value outside the mixing zone. It should be noted that since these curves are plotted with R as the independent variable, the actual curves in physical coordinates show a rapidly expanding hot bubble, surrounded by a mixing zone, which is itself thickening with time. This explains how the gas well inside the

flame brush is heated, even though the velocity field is always directed outward. In fact, all the gas inside the flame brush has already passed through it.

Finally, the pressure rise above ambient is found from the momentum Eq. (2). The solution takes the form:

$$P - p_\infty = \rho_\infty (V\beta)^2 P(R), \quad (18)$$

$$P = \int_R^\infty B(R) \left(W - \frac{R}{\beta} \right) \frac{dW}{dR} dR. \quad (19)$$

This result is basically a generalization of the classical Bernoulli equation for time dependent potential flows. Indeed, outside the flame brush the density ratio $B = 1$, and Eq. (19) can be integrated to yield:

$$P + \frac{W^2}{2} - \frac{1}{\beta} \left(RW + \int_R^\infty W dR \right) = 0. \quad (20)$$

The term in round brackets in Eq. (20) is proportional to the negative of the time derivative of the velocity potential ϕ , defined so that:

$$\phi = -\beta V^2 t \int_R^\infty W dR. \quad (21)$$

The dimensionless pressure rise $(p - p_\infty)/(\rho_\infty (V\beta)^2)$ is plotted in Fig. 2. It consists of a long slow decay from a peak centered just outside the flame brush. This decay is described by the time dependent Bernoulli equation (20), since the density takes on its ambient value in this region. The peak values of the excess pressure are only weakly dependent on the temperature ratio behind the flame brush, with higher temperatures corresponding to slightly smaller values of the pressure rise. This behavior occurs because it takes less force to push out a lower density gas, and because most of the force is required to push out the large mass of cold gas surrounding the hot bubble.

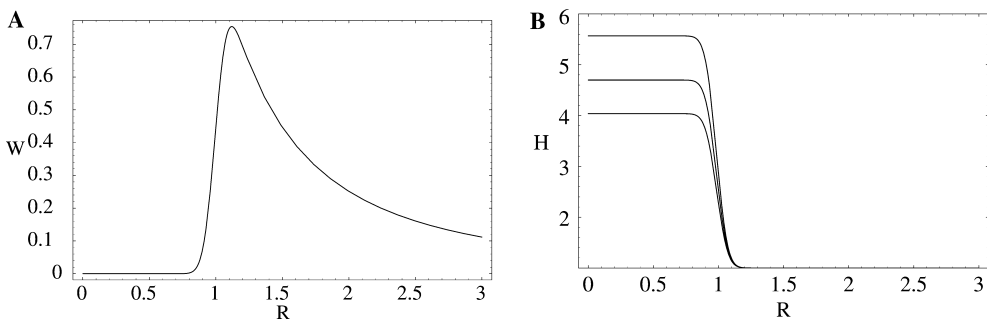


Fig. 1. Dimensionless radial expansion velocity $W = v/(\beta V)$ (A) and enthalpy ratio $H = h/h_\infty$ (B) plotted as function of similarity variable $R = r/(Vt)$. The curves for h/h_∞ correspond to values $\beta = 0.85, 0.90,$ and 0.95 , with increasing values generating higher peak enthalpy.

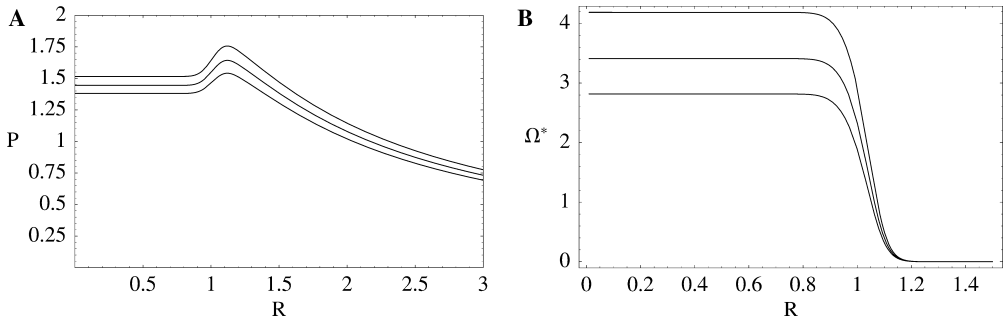


Fig. 2. Dimensionless pressure rise $P = (p - p_\infty)/(\rho_\infty (V\beta)^2)$ (A) and vorticity function $\Omega^* = \omega V/(g \sin \theta)$ (B) plotted as function of similarity variable $R = r/(Vt)$. The curves correspond to values $\beta = 0.85, 0.90,$ and 0.95 , with increasing values generating higher Ω^* but lower P .

4. Buoyancy induced flow

The solenoidal component of the velocity field arises entirely because of the buoyancy induced by the heat release. Eq. (6) determines the vorticity distribution, from which the solenoidal velocities are obtained. Since the density ratio B depends only on R , we seek a solution consistent with that functional dependence. This can be accomplished by introducing a function $\Omega(R)$ defined such that:

$$\omega = \frac{g}{V} \sin \theta R B \Omega = \frac{g}{V} \sin \theta \Omega^*(R). \tag{22}$$

The function $\Omega(R)$ is then a solution of the following equation:

$$(R - \beta W) \frac{d\Omega}{dR} + \Omega = -\frac{1}{B^3} \frac{dB}{dR}. \tag{23}$$

Given the functional form for the vorticity shown in Eq. (22), it is easy to show that the buoyancy induced flow field is initially small compared with the expansion velocity. Since the vorticity is related to the solenoidal velocity components (u_r, u_θ) by Eq. (7), the spatial and temporal dependence of these components must be of the form $gt(U_r(R, \theta), U_\theta(R, \theta))$, where U_r and U_θ are dimensionless velocity components. Thus, the buoyancy induced flow grows initially from rest, while the expansion velocity in the flame brush is always $O(\beta V)$. This also implies that the initial vertical motion of the fireball as a whole is proportional to gt^2 . Thus, the fireball rise will not become apparent until $gt^2 \approx Vt$.

The solution for Ω is readily found to be:

$$\Omega = \int_R^\infty f_3(R_1) \exp[-I_2(R_1, R)] dR_1, \tag{24}$$

$$f_3 = \frac{1}{B^3(R_1)} \frac{dB}{dR_1} \frac{1}{(R_1 - \beta W(R_1))}, \tag{25}$$

$$I_2 = \int_{R_1}^R \frac{dR_o}{(R_o - \beta W(R_o))}. \tag{26}$$

The vorticity function Ω^* is shown in the right-hand plot of Fig. 2. It is qualitatively similar to the plot for the enthalpy ratio H . This is not accidental, since the vorticity and temperature rise are both created in the flame brush and convected by the expansion velocity. As a result, both are confined to the region in and behind the flame brush, and decay rapidly ahead of it. The important difference is that the vorticity itself is a component of a vector field, which is not spherically symmetric. Indeed, the solenoidal velocity field cannot be spherically symmetric, since such a velocity field contains no vorticity.

The final step in the analysis is the determination of the buoyancy induced velocity itself. This is accomplished by solving Eq. (9) for the function ψ . Again using the functional form for the vorticity expressed in Eq. (22), Eq. (9) can be rewritten in the form:

$$\frac{\partial^2 \Psi}{\partial R^2} + \frac{\sin \theta}{R^2} \frac{\partial}{\partial \theta} \left(\frac{1}{\sin \theta} \frac{\partial \Psi}{\partial \theta} \right) = -\sin^2 \theta R \Omega^*(R). \tag{27}$$

Here, Ψ is a dimensionless “stream function” related to ψ as follows:

$$\psi = (Vt)^3 \frac{g}{V} \Psi(R, \theta). \tag{28}$$

The solution to Eq. (27) can be readily found by noting that Ψ must take the form:

$$\Psi = \sin^2 \theta F(R). \tag{29}$$

The unique solution consistent with the requirements that F be finite at $R=0$ and vanish as $R \rightarrow \infty$ is:

$$F(R) = \frac{1}{3R} I_3(R) + \frac{R^2}{3} I_4(R), \tag{30}$$

$$I_3 = \int_0^R R_o^3 \Omega^*(R_o) dR_o, \tag{31}$$

$$I_4 = \int_R^\infty \Omega^*(R_o) dR_o. \quad (32)$$

Examination of the properties of the vorticity function Ω^* (see the right-hand plot in Fig. 2) shows that since Ω^* is finite as $R \rightarrow 0$, the first integral in Eq. (30) vanishes $\sim R^4$. Moreover, $\Omega^* \rightarrow 0$ exponentially outside the flame brush. Thus, both integrals are well behaved, and the function $F(R)$ has the desired properties.

Figure 3 shows contours of the dimensionless vorticity $\omega V/g$ and stream function Ψ . The buoyancy induced vortex is clearly apparent in both plots. The induced velocities decay $\sim R^{-3}$ far from the expanding bubble. The induced velocity is directed upwards along the axis of symmetry. Thus, while the streamlines are symmetrical with respect to the horizontal plane $R \cos \theta = 0$, the induced velocities are not. The solution is symmetric with respect to any vertical plane passing through $R = 0$. Thus, it is a suitable inviscid model for either a spherically symmetric fireball in an unbounded space or a hemispherical fireball emerging from a hole in a vertical wall.

Finally, the role of thermal radiation will be briefly noted. The fireball unquestionably emits thermal radiation as it expands. Indeed, for a spherical fireball the initial radiant energy flux q_r can be determined from an optically thin analysis as the solution to the equation:

$$\frac{1}{r^2} \frac{\partial}{\partial r} (r^2 q_r) = 4\kappa\sigma(T^4 - T_\infty^4). \quad (33)$$

Here, κ is the grey gas absorption coefficient (dominated by soot particulate for all but the cleanest fuels) and σ is the Stefan–Boltzmann constant. However, when the equation is recast with R as independent variable and the integration carried out, the result is readily found to be:

$$q_r = \frac{4\sigma V t}{R^2} \int_0^R R_o^2 \kappa(R_o) (T^4(R_o) - T_\infty^4) dR_o. \quad (34)$$

This result shows that the radiant energy flux builds up linearly from zero with increasing time. Hence, its contribution to the initial energy balance is small compared with the combustion and radial convective transport. Thus, it is entirely consistent to ignore radiation in the initial energy balance in the gas, even though radiant energy will be emitted as soon as the fireball is ignited.

5. The WTC fireball

Using the photographs and video material collected by the National Institute of Standards and Technology (NIST) as part of its WTC investigation, we have been able to estimate the growth of the South-Tower fireballs as a function of time. Several videos were used because videos were taken from different directions and at different distances from the WTC complex. Videos were examined frame by frame, with times determined relative to the initial impact of the plane. Lengths were determined on each frame relative to the width of a tower face, 63.1 m long, adjusted for viewing angle of the video.

First, we note that the South-Tower fireballs appeared only on three faces of WTC2, the south, east, and north faces. (Window breakage, and, therefore hot-gas escape, on the west face only appeared after this initial transient.) The normal distance of the fireball from each face was plotted as a function of time, as shown, along with a photograph characteristic of the fireball, in Fig. 4. The line superimposed on this plot of the data was determined by a least-squares fit, yielding a value of about 28 m/s for the growth speed of the fire-

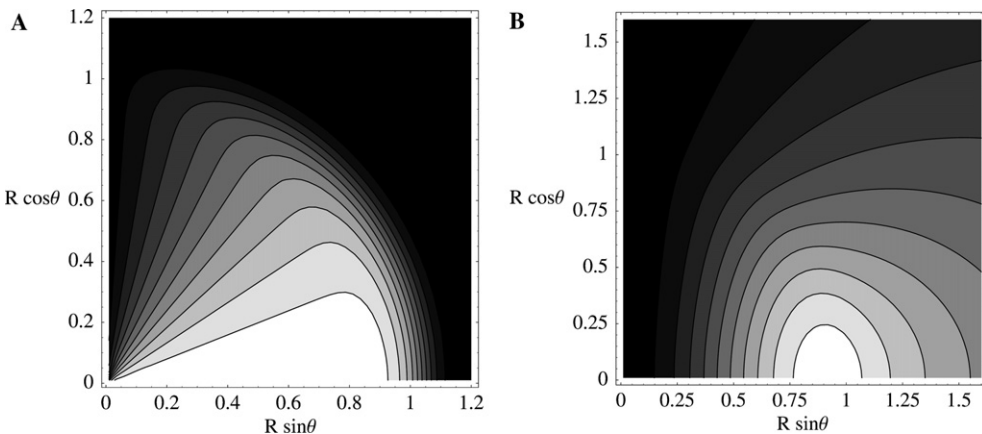


Fig. 3. Dimensionless buoyancy induced vorticity contours (constant $\omega V/g$, A) and streamlines of buoyancy induced flow (constant Ψ , B) for $\beta = 0.9$. The contours shown correspond to the upper half of the expanding bubble and are symmetric with respect to the plane $R \cos \theta = 0$.

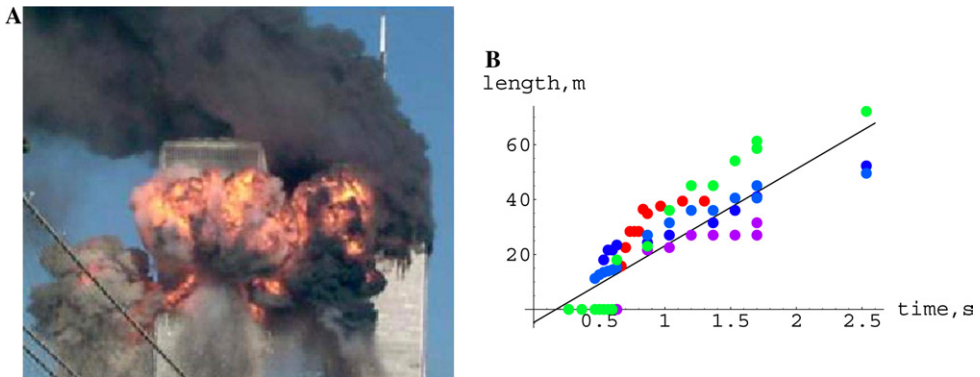


Fig. 4. Photograph of South Tower fireball (©2001 Sara K. Schwittek. All rights reserved. Used by permission) (A), shortly after collision with second plane. Estimates of fireball radial extent taken from five sets of video images (B). The straight line fit corresponds to an expansion velocity $V = 28$ m/s.

ball. The scatter in the data gives an estimate of the error involved in this procedure.

Given an estimate of the expansion velocity V and the fact that physically plausible values of the parameter β fall in the range, $0.85 \leq \beta \leq 0.95$, the midrange choice yields an estimate $q = 0.9 \text{ MW/m}^2$. This heat release rate per unit area of nominal flame front is similar to the heat release rate per unit area for hydrocarbon pool fires. Adding up the contributions of the three fireballs and integrating over the 2.5 s that elapse before the fireballs begin to rise give an estimate of 1.6×10^3 kg of fuel consumed, assuming the energy content of the fuel to be 43 MJ/kg. This result should be considered a lower bound on the fuel consumption in the fireball for at least two reasons. First, it assumes complete combustion of the fuel. Second, it takes no account of the additional burning that occurred after the fireballs began to rise. This result is consistent with results based on the CFD simulations displayed in Fig. 6 of [8]. These calculations reproduce the fireball shown in Fig. 4 quite accurately for assumed total fuel burns varying from 10% to 25% of the estimated fuel load of 2.8×10^4 kg carried by the plane. In fact, if the time spanned was extended to 3–4 s (which ignores the increasingly important effects of fireball merging and buoyancy), then the fuel consumed in the fireballs according to this model would completely overlap the CFD based predictions of [8]. Thus, most of the fuel was available to serve as an ignitor for the fires that helped to destroy these buildings.

6. Concluding remarks

A simple model of the initial development of a fireball has been presented. The chief simplification is the assumed form of the spatial and temporal distribution of the heat release rate. Given this assumed form, the mass, momentum, and energy

conservation equations are solved exactly. The solutions depend on two parameters, ϵ and β . The first of these determines the ratio of the flame brush thickness to the overall fireball radius, while the second is the ratio of the local heat release rate to the available enthalpy flux per unit area of flame brush.

Clearly, in a detailed CFD based simulation that included both a high resolution analysis of the mixing in the flame brush and an explicit combustion model, local quantities equivalent to ϵ and β would be part of the output. However, detailed CFD simulations require a large amount of input information (as well as a lot of computation). Unless this information is both available and accurate, the additional detail provided in principle by a CFD based simulation may prove illusory in practice. The present model, in contrast, primarily requires a plausible estimate for β in order to be in a position to extract useful information from an accident scenario. Moreover, the results obtained above show that physically interesting values of β are strongly constrained by the solutions to the conservation equations. Thus, given video information, the expansion velocity V can be extracted. Since β is strongly constrained, a knowledge of V leads directly to an estimate for the heat release per unit area q , and thus to the global energy release rate. This procedure yields a useful lower bound for the fuel consumption in the WTC fireballs. Hopefully, it can be used for other purposes as well.

References

- [1] G.M. Makhviladze, S.E. Yakush, *Proc. Combust. Inst.* 29 (2002) 195–210.
- [2] J.A. Fay, D.H. Lewis, *Proc. Combust. Inst.* 16 (1976) 1397–1405.
- [3] G.M. Makhviladze, J.P. Roberts, S.E. Yakush, in: Y. Hasemi (Ed.), *Fire Safety Science—Proceedings*

- of the *Fifth International Symposium, IAFSS*, 2001, pp. 213–224.
- [4] G.M. Makhviladze, J.P. Roberts, S.E. Yakush, *Combust. Flame* 118 (4) (1999) 581–605.
- [5] R.G. Rehm, H.R. Baum, *J. Res. Natl. Bur. Stand.* 83 (1978) 297–308.
- [6] G.M. Makhviladze, S.E. Yakush, *Proc. Combust. Inst.* 29 (2002) 313–320.
- [7] G. Corley, R. Hamburger, T. McAllister, in: T. McAllister (Ed.), *World Trade Center Building Performance Study: Data Collection, Preliminary Observations, and Recommendations*, Report FEMA 403, May 2002, p. 1.
- [8] R.G. Rehm, W. Pitts, H.R. Baum, D.D. Evans, K. Prasad, K.B. McGrattan, G.P. Forney, *Initial Model for Fires in the World Trade Center Towers*, Report NISTIR 6879, National Institute of Standards and Technology, May 2002.
- [9] I. Glassman, *Combustion*, second ed. Academic Press, Orlando, FL, 1987, p. 439.
- [10] S. Goldstein, *Lectures on Fluid Mechanics*. Interscience, New York, 1960, pp. 73–76.
- [11] S. Goldstein, *Lectures on Fluid Mechanics*. Interscience, New York, 1960, pp. 27–31.
- [12] H.R. Baum, in: D. Bradley, D. Drysdale, G. Makhviladze (Eds.), *Fire and Explosion Hazards, Proceedings of the Third International Seminar*, University of Central Lancashire, Preston, Lancashire, 2001, pp. 3–22.
- [13] H.R. Baum, W.E. Mell, *Proc. Combust. Inst.* 28 (2000) 473–479.

Comment

James G. Quintiere, University of Maryland, USA. 1. The initial condition for your WTC fireball problem is a premixed deflagration vented explosion. The pressures resulting from this bears on the damage, especially to the steel insulation; have you considered those effects, and could they be important?

2. Your elegant model does not include the effect of oxygen entrainment, or combustion, as do other fireball theories and correlations (e.g., Fay et al.). Have you compared your model to those simpler fireball data sets to assess the accuracy and advantage of your new solution?

Reply. The whole point of the present analysis is to develop a description of the fireball that does *not* depend on interior details. For example, it is far from clear that the fireball starts as a “premixed deflagration.” In fact, the CFD analysis of the fireball described ([8] in paper) uses the NIST Fire Dynamics Simulator (FDS). FDS treats the fireball as a non-premixed deflagration using

a mixture fraction formulation. As noted in the text above and in Fig. 6 of ([8] in paper), the computed results reproduce the observed fireball quite well given plausible assumptions about the interior geometry and fuel distribution.

The assertion that the model “does not include the effect of oxygen entrainment or combustion” is incorrect. A mixing layer whose thickness grows with time as the fireball expands represents the heat release zone. The quantities being mixed are fuel and air. Indeed, it is easy to show that an oxygen mass fraction equation with the heat release related to oxygen consumption by Huggetts rule produces a steady depletion of oxygen as the mixing layer is traversed. Analyses like that of Fay and Lewis ([2] in paper) are concerned with the rise of a spherical fireball, and contain far less physics than the present model. We have correlated our model with the fireball “data” that emerges from the actual WTC events. That is what this paper is about.